Vortex trapping of sand grains over ripples under oscillatory flow

D. Frank-Gilchrist *U.S. Geological Survey - St. Petersburg Coastal and Marine Science Center, St. Petersburg, Florida, USA - dfrank-gilchrist@usgs.gov*
A. Penko *U.S. Naval Research Laboratory, Stennis Space Center, Mississippi, USA - allison.penko@nrlssc.navy.mil*
M. Palmsten *U.S. Geological Survey - St. Petersburg Coastal and Marine Science Center, St. Petersburg, Florida, USA - mpalmsten@usgs.gov*
J. Calantoni *U.S. Naval Research Laboratory, Stennis Space Center, Mississippi, USA- joe.calantoni@nrlssc.navy.mil*

ABSTRACT: Sand ripples significantly impact morphodynamics in the nearshore by generating coherent vortices, which can transport suspended sediment to greater heights in the water column than above flat beds. Coherent vortices can trap sediment grains if the settling velocity of the grain is smaller than the maximum vertical fluid velocity in the vortex (Nielsen 1992). Particle image and tracking velocimetry were used to measure small-scale fluid-sediment interactions over sand ripples in a small oscillatory flow tunnel. Here we present some of the first measurements of vortex-trapped sediment grains under oscillatory flows. Results showed that the vortex-trapped sand grain traversed an orbit off-center of the vortex near the ripple slope. Some grains then spiralled outward and settled to the bed; others were transported by the flow as the vortex was shed from the crest. Vortex trapping can delay settling and increase settling times, potentially causing inaccurate sediment transport predictions by large-scale numerical models, which do not typically account for this non-linear small-scale process.

1 INTRODUCTION

Sand ripples impact hydrodynamics and morphodynamics in the nearshore. For example, fluid velocities above ripple crests may be up to two times faster than the freestream (Van der Werf et al., 2007; Frank-Gilchrist et al., 2018). The hydrodynamics of the flow up to twice the ripple height above the ripple crest are dominated by coherent vortices, formed on the ripple slopes and ejected into the water column at flow reversal (Davies and Villaret, 1997; Rodríguez-Abudo et al., 2013).

The coherent vortices, shed from ripples, transport sediment as suspended load to greater heights in the water column than above flat beds (Van der Werf et al., 2006; Nichols and Foster, 2007; Frank-Gilchrist et al., 2018). Coherent vortices also trap sediment grains when the settling velocity of the sediment grain is smaller than the maximum upward fluid velocity in the vortex (Nielsen 1992). Under these conditions, the grain would traverse an orbit off-center of the vortex before spiraling outward and eventually settling to the bed or being transported by the flow. This can cause increased settling time, making vortex trapping an important mechanism that may affect sediment transport in coastal regions. The lack of delayed settling in models may lead to inaccurate predictions of bedform evolution, estimates of bed shear stresses, and consequently large-scale sediment transport processes impacting coastal regions.

In this study, one of the first observations of vortex trapping of sediment grains under oscillatory flows is presented. Measurements of small-scale fluid-sediment interactions by Frank-Gilchrist et al. (2018) were further analyzed for oscillatory flow conditions under which vortex trapping was observed. Qualitative comparisons with the vortex trapping hypothesis of Nielsen (1992) are also described.

2 EXPERIMENTAL METHODS

High-resolution experiments were conducted in the Small Oscillatory Flow Tunnel (S-OFT) at the U.S. Naval Research Laboratory at Stennis Space Center, Mississippi, USA. The test section is 2 m long with a flow cross-section of 0.25×0.25 m (Calantoni et. al, 2013). Oscillatory flow was generated with a piston and flywheel assembly to drive sediment transport and ripple formation (Frank-Gilchrist et al., 2018). The rippled bedforms were comprised of well-sorted, coarse quartz sand with a median grain diameter of 0.7 mm and density of 2,650 kgm^{-3}.

Phase-separated particle image velocimetry (PIV) and particle tracking velocimetry (PTV) were used to measure three-dimensional fluid velocities and two-dimensional sediment velocities in the oscillatory bottom boundary layer in a two-dimensional vertical plane of the water column. A downward-looking Nd: YAG laser was mounted above the test section to produce the 2 mm light sheet. Optical filters were installed on two high-speed cameras, set up in stereographic mode, to capture the light re-emitted at a higher wavelength by the fluorescent tracer particles (Figure 1). A neutral density filter was installed on the third camera, centered in the test section, to capture the light scattered by the sediment grains. The overlapping, simultaneously recorded images provided sediment particle and fluid velocities at high temporal (100 Hz) and spatial (≤ 1 mm) resolution. Further details of the experimental setup are described in Frank-Gilchrist et al. (2018).

The PIV images captured by the two outer cameras were processed with the LaVision software, DaVis (LaVision 2014) to calculate the three components of fluid velocity. The images captured by the center camera were used to calculated the mean image to represent the background intensity. The particle finder algorithm determined areas of contrast that had higher intensity than the background, given a threshold intensity (Ouellette, 2010). Contiguous areas of laser light intensity scattered by the grains that were higher than the threshold intensity count and larger than the minimum area of pixels representing the imaged sediment grain, were compared with the raw camera images to verify that sediment grains were detected. The centroid for each contiguous area of light was calculated to determine the location coordinates for each sediment grain (Ouellette, 2010). The grain location

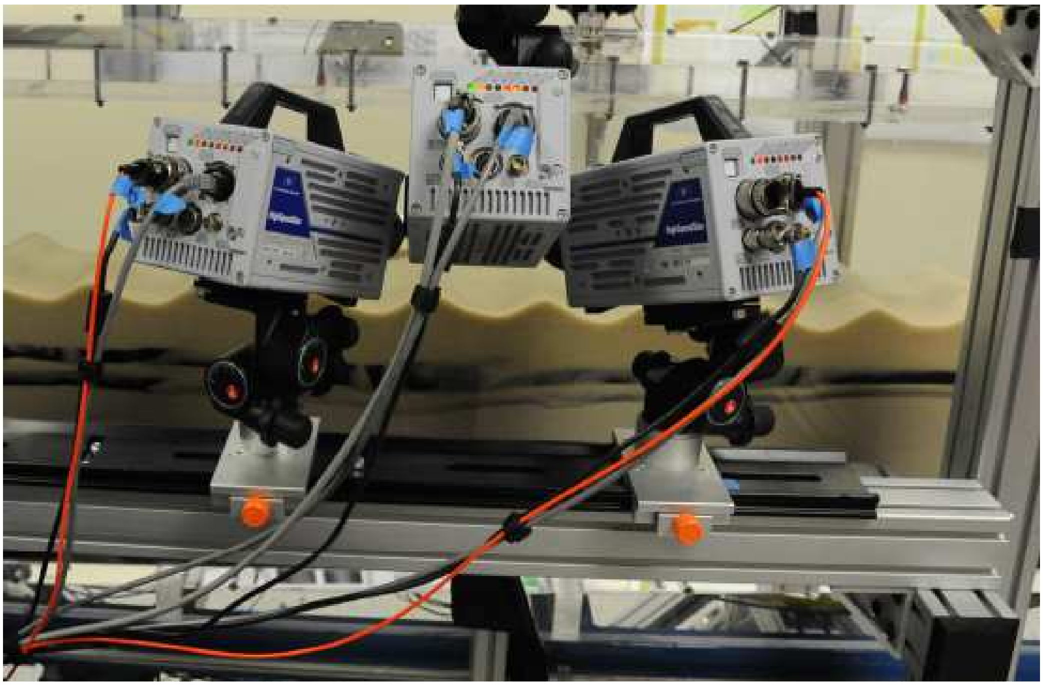

Figure 1. Experimental setup of particle image and tracking velocimetry system in the Small-Oscillatory Flow Tunnel at the U.S. Naval Research Laboratory, MS.

coordinates and estimated maximum displacement of the sediment grains between time steps were used by a particle tracking algorithm (Ouellette et al., 2006) to distinguish the sediment grains and determine the associated trajectories. The sediment grain trajectories were then compared with the vortex trapping hypothesis of Nielsen (1992).

3 RESULTS & DISCUSSION

Two-dimensional ripples were generated in the oscillatory flow tunnel, and high-resolution measurements of fluid-sediment interactions were made to assess sediment transport mechanisms over the sand ripples. The two-dimensional ripples generated in the oscillatory flow tunnel had a wavelength of 0.13 m and a ripple height of 0.025 m (Frank-Gilchrist et al., 2018). Here, we present preliminary results of one instance in which vortex trapping was observed during the experiment. The oscillatory flow period, T, was 2.35 s and the orbital velocity amplitude, U_o, was 0.26 ms^{-1}. The raw flow velocities were smoothed temporally and spatially to reduce noise and improve data quality. The velocities were then used to calculate the flow vorticity to better illustrate the location of the vortex relative to the vortex-trapped grain.

Figure 2 illustrates smoothed fluid velocities throughout the first half of the flow cycle. After flow reversal, the flow velocities were very small across the domain except for the extreme right side where a region of higher negative velocities was captured on the opposite side of the adjacent ripple (Figure 2(b)). As the freestream velocity accelerated, the nearbed velocity along the

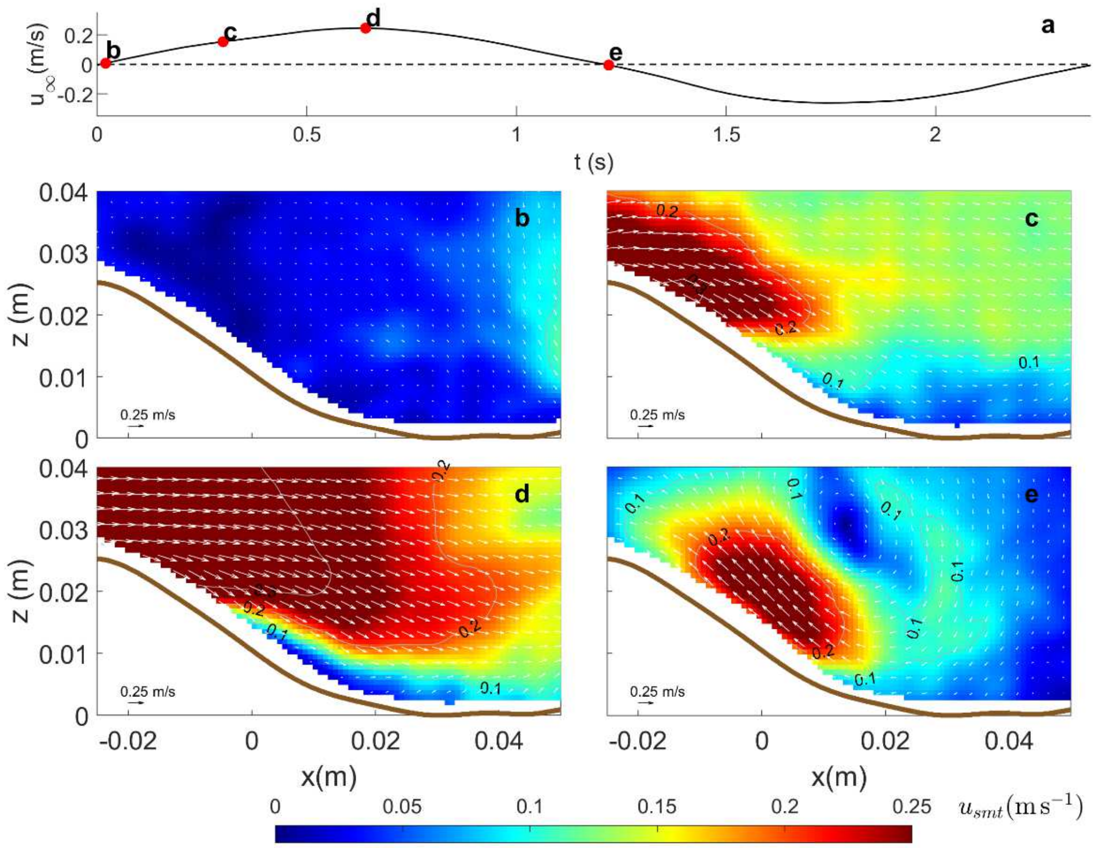

Figure 2: Time series of free-stream velocity is shown in panel (a). Fluid velocities are overlaid on color plots of velocity magnitude for the right half of the ripple, shown as white arrows in panels (b) – (e), at corresponding time steps indicated in panel (a). A scale vector is indicated in the bottom left corner of panels (b) – (e). The brown line delineates the average ripple shape for this trial.

ripple slope increased to a similar magnitude as the peak freestream velocity (Figure 2(c)). By the time of maximum freestream velocity, the flow across the domain had also increased significantly (Figure 2(d)). During the decelerating phase of the flow, the fluid velocities indicate a circular region of low velocity surrounded by fluid of higher velocity, suggesting the formation of a vortex just prior to flow reversal. (Figure 2(e)). The observed flow dynamics are in agreement with measurements by Van der Werf et. al (2007) of flow velocities over sand ripples, among others.

The panels shown in Figure 3(b) – (d) were taken just before the flow reversed from positive to negative when the cameras captured vortex generation on the ripple slope. For the time steps shown, the vortex diameter, estimated with a circle fit algorithm (Chernov, 2017), ranged from 0.024 – 0.03 m, of similar magnitude to the height of the vortex ripple. Some sediment grains were observed to prescribe semi-circular trajectories. The semi-circular path was off-center of the vortex core in the quadrants closer to the ripple slope, as hypothesized by Nielsen (1992) for vortex-trapped grains.

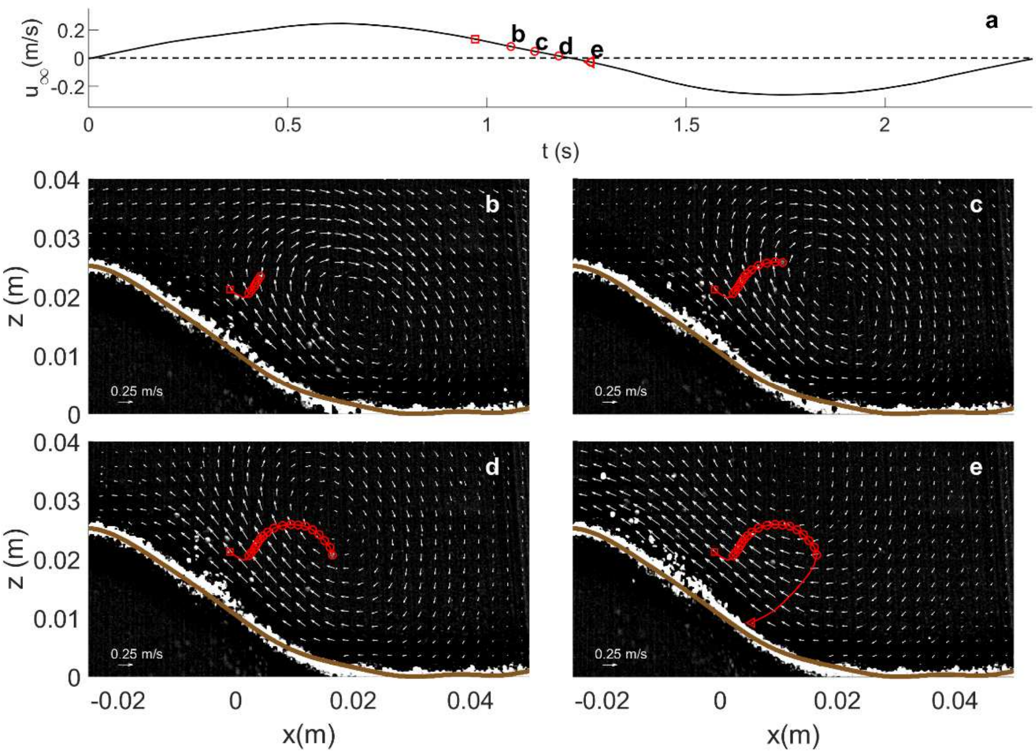

Figure 3: Time series of freestream velocity is shown in panel (a). Instantaneous velocities vectors are overlaid on PIV images of the right side of the ripple, shown as white arrows in panels (b) – (e) at corresponding time steps indicated in panel (a). A scale vector is indicated in the bottom left corner of panels (b) – (e), and the brown line delineates the average shape of the ripple bed for this trial. Shown in panels (b) – (e) is the trajectory of a vortex-trapped sand grain that traversed a semicircular path. The start and end times of the entire trajectory are indicated by red square and triangle symbols in panel (a), respectively. The time steps for the snapshot are indicated with sold circles in panel (a). The semi-circular portion of the trajectory is also indicated with circular markers in panels (b) – (e).

The grain highlighted in red was first mobilized and advected with the flow before being trapped in the vortex, illustrated by the initial straighter portion of the sediment grain trajectory (Figure 3(b)). As the grain began to settle, it interacted with the upward velocities of the vortex and was temporarily trapped in the vortex resulting in a change of direction, illustrated by the circular portion of the trajectory indicated with the circle markers (Figure 3(b-d)). The initial and final straight portions of the grain trajectory differ from the purely circular path hypothesized by Nielsen (1992) because the grain was being advected during these times rather than being trapped in the vortex. In addition, the vortices observed in these experiments were not stationary but were generated, advected then dissipated with each oscillatory flow cycle.

Next, the vorticity of the flow was calculated to determine the strength of the vortex. The smoothed and temporally averaged fluid velocities were used to calculate the vorticity to reduce the effects of small-scale turbulence and noise in the data. The time-varying vorticity, ω_v, was

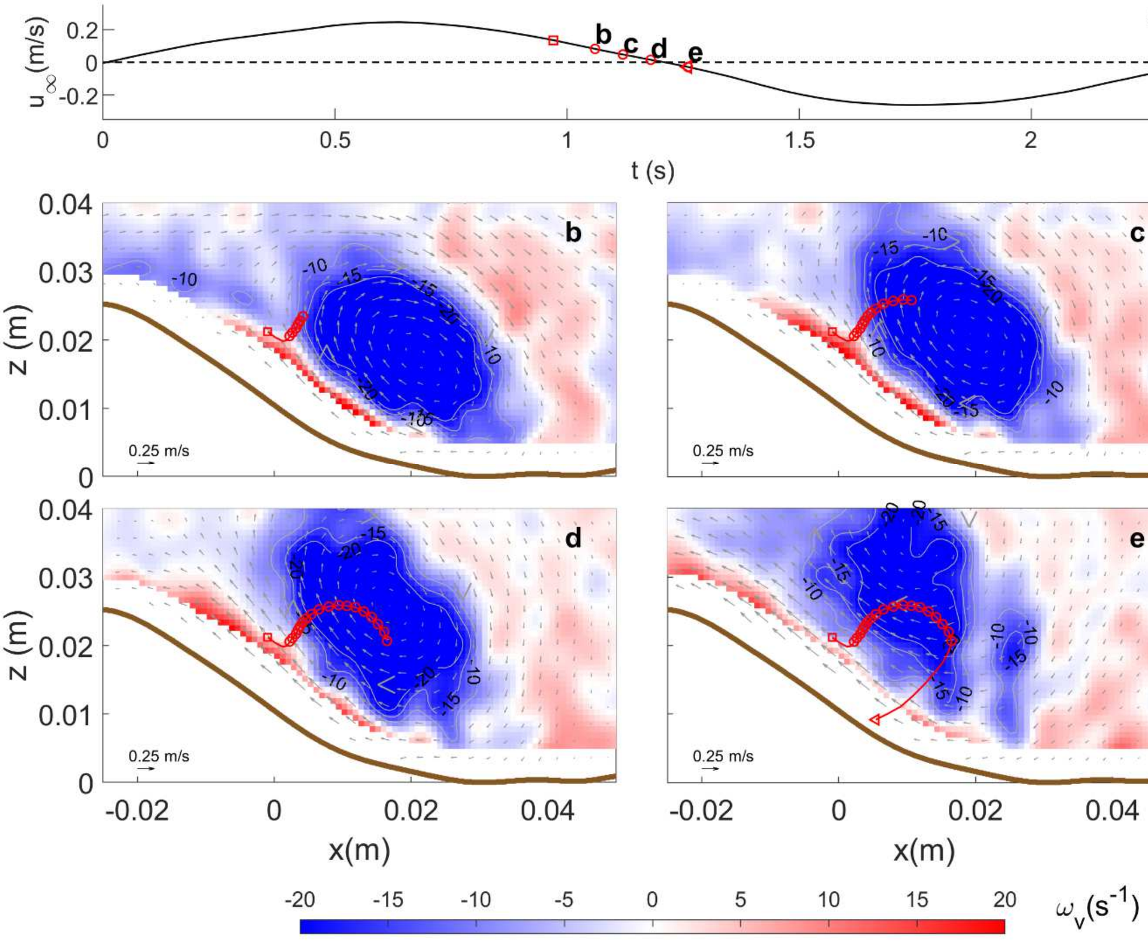

Figure 4: Time series of freestream velocity is shown in panel (a). Instantaneous velocities are overlaid on contour plots of vorticity for the right side of the ripple, shown as gray arrows in panels (b) – (e) at corresponding time steps indicated in panel (a). A scale vector is indicated in the bottom left corner of panels (b) – (e), and the brown line delineates the average shape of the ripple bed for this trial. Shown in panels (b) – (e) is the trajectory of a vortex-trapped sand grain that traversed a semicircular path. The start and end times of the entire trajectory are indicated by red square and triangle symbols in panel (a), respectively. The time steps for the snapshot are indicated with sold circles in panel (a). The semi-circular portion of the trajectory is also indicated with circular markers in panels (b) – (e).

calculated as the curl of the smoothed velocity field (Sveen, 2004; Nichols and Foster, 2007) (Figure 4). The observed vortex was asymmetric with the strongest vorticity in the upper left quadrant near the bed compared with the quadrants of the vortex that were closer to the freestream. The asymmetry of the vortex may be due to the flattened trough of the sand ripples that were generated in the oscillatory flow tunnel as opposed to the rounded concave shape that is more typical of sand ripples in the nearshore. This may have been due to a slight asymmetry in the forcing of the piston-flywheel assembly driving the oscillatory flow.

Figure (4) illustrates that the sediment grain was trapped near the region of higher vorticity. During the decelerating phase of the flow just after the maximum freestream velocity, the vortex was being generated and was still attached to the ripple slope (Figure 4b). Later in the flow cycle prior to flow reversal, the vortex had fully developed and was being advected with the flow before being shed from the ripple crest (Figure 4 (c-e). Although no measurements were made on the other side of the ripple during the opposite flow reversals for this trial, similar vortex development and flow dynamics were observed, as expected for the symmetric oscillatory flow.

This effort is ongoing and further analyses will be performed for this rich dataset. The trajectories will be determined for other sediment grains that were observed to prescribe semi-circular paths, as expected for vortex-trapped grains. In addition, the sediment grain velocities will be compared with the fluid velocities to perform quantitative comparisons with the vortex-trapping hypothesis of Nielsen (1992).

4 CONCLUSIONS

High-resolution measurements of fluid-sediment interactions over natural sand ripples under oscillatory flows were analyzed to assess an observation of a vortex-trapped sediment grain. Coherent structures were identified and determined to be a significant mechanism for mobilizing and transporting suspended sediments. The vortex-trapped grain was observed to move in a counterclockwise motion within the quadrants of the vortex closest to the ripple slope, in agreement with Nielsen (1992).

These results represent one of the first observations of vortex trapping of coarse sand grains over sand ripples under oscillatory flows. Vortex trapping is an important mechanism for sediment transport under these hydrodynamic conditions. Including vortex trapping in settling velocity calculations could improve sediment transport predictions in larger-scale numerical models.

5 ACKNOWLEDGEMENT

Donya Frank-Gilchrist was supported by the National Research Council Research Associateship Program at the Naval Research Laboratory Stennis Space Center when the experiments were conducted. Subsequent analyses were performed while Donya Frank-Gilchrist and Margaret Palmsten were affiliated with the U.S. Geological Survey St. Petersburg Coastal and Marine Science Center. Allison Penko and Joseph Calantoni were supported under base funding to the United States Naval Research Laboratory from the Office of Naval Research. The authors would like to acknowledge technical staff members at the United States Naval Research Laboratory for their assistance with experimental setup and data collection. This information is preliminary and is subject to revision. It is being provided to meet the need for timely best science. The information is provided on the condition that neither the U.S. Geological Survey nor the U.S. Government shall be held liable for any damages resulting from the authorized or unauthorized use of the information. Any use of trade, firm, or product names is for descriptive purposes only and does not imply endorsement by the U.S. Government.

6 REFERENCES

Calantoni, J., B. J. Landry, and A. M. Penko, 2013, Laboratory observations of sand ripple evolution using bimodal grain size distributions under asymmetric oscillatory flows. Journal of Coastal Research, 65, 1497–1502. https://doi.org/10.2112/SI65-253.1

Chernov, N., 2017, Circle Fit (Taubin method). (https://www.mathworks.com/matlabcentral/fileexchange/22678-circle-fit-taubin-method) MATLAB Central File Exchange. Retrieved September 2017.

Davies, A. G., and C. Villaret (1997), Oscillatory flow over rippled beds: Boundary layer structure and wave-induced Eulerian drift. International Series On Advances in Fluid Mechanics, 10 pp. 215-254.

Frank-Gilchrist, D., A. Penko, and J. Calantoni (2018), Investigation of sand ripple dynamics with combined particle image and tracking velocimetry. Journal of Atmospheric and Oceanic Technology, 35 (10), 2019–2036. https://doi.org/10.1175/JTECH-D-18-0054.1

LaVision, 2014: FlowMaster Product-Manual for DaVis 8.2. LaVision Rep., 188 pp.

Nichols, C. S., and D. L. Foster, 2007: Full-scale observations of wave-induced vortex generation over a rippled bed. Journal of Geophysical Research, 112. https://doi.org/10.1029/2006JC003841

Nielsen, P. (1992). Coastal bottom boundary layers and sediment transport. World Scientific, Singapore, 324pp.

Ouellette, N. T., Xu, H., and Bodenschatz, E. (2006), A quantitative study of three-dimensional Lagrangian particle tracking algorithms. Experiments in Fluids, 40 (2), 301–313.

Ouellette, N. T. (2010), Particle Tracking. Ouellette Lab. https://web.stanford.edu/nto/software tracking.shtml,. Accessed 12 September 2017.

Rodríguez-Abudo, S., D. Foster, and M. Henriquez, 2013, Spatial variability of the wave bottom boundary layer over movable rippled beds. Journal of Geophysical Research: Oceans, 118 (7), 3490–3506. https://doi.org/10.1002/jgrc.20256

Sveen, J.K. (2004), An introduction to MatPIV 1.6.1, 2nd ed., report. Department of Mathematics, University of Oslo, Oslo. pp. 1-27.

Van der Werf, J.J., Ribberink, J.S., O'Donoghue, T., and Doucette, J.S. (2006), Modelling and measurement of sand transport processes over full-scale ripples in oscillatory flows. Coastal Engineering, 53, 657–673. https://doi.org/10.1016/j.coastaleng.2006.02.002

Van der Werf, J.J., Doucette, J.S., O'Donoghue, T., and Ribberink, J.S. (2007), Detailed measurements of velocities and suspended sand concentrations over full-scale ripples in regular oscillatory flow. Journal of Geophysical Research: Earth Surface,112 (F2). https://doi.org/10.1029/2006JF000614